Dynamic Medicine

Research

Regulation of oxygen transport during brain activation: stimulus-induced hemodynamic responses in human and animal cortices

Akitoshi Seiyama*[1,2], Junji Seki[3], Hiroki C Tanabe[1], Yasuhiro Ooi[4], Yasuhiko Satomura[2,3], Hisao Fujisaki[5] and Toshio Yanagida[1,2]

Address: [1]Kansai Advanced Research Center, Communications Research Laboratory, 588-2 Iwaoka, Nishi-ku, Kobe, Hyogo 651-2492, Japan, [2]Division of Physiology and Biosignaling, Osaka University Graduate School of Medicine, 2-2 Yamadaoka, Suita, Osaka 565-0871, Japan, [3]Department of Biomedical Engineering, National Cardiovascular Center Research Institute, 5-7-1 Fujishiro-dai, Suita, Osaka 565-8565, Japan, [4]Division of Pathogenesis and Control of Oral Disease, Osaka University Graduate School of Dentistry, 1-8 Yamadaoka, Suita, Osaka 565-0871, Japan and [5]Nikon Corp. Business Development Center, 1-6-3 Nishi-Ooi, Shinagawa, Tokyo 140-8601, Japan

Email: Akitoshi Seiyama* - aseiyama@po.crl.go.jp; Junji Seki - sekij@ri.ncvc.go.jp; Hiroki C Tanabe - htanabe@nips.ac.jp; Yasuhiro Ooi - osa-musi-kps@iam.ne.jp; Yasuhiko Satomura - satomura@phys1.med.osaka-u.ac.jp; Hisao Fujisaki - fujisaki.h@nikon.co.jp; Toshio Yanagida - yanagida@phys1.med.osaka-u.ac.jp

* Corresponding author

Abstract

Background: The correlation between regional changes in neuronal activity and changes in hemodynamics is a major issue for noninvasive neuroimaging techniques such as functional magnetic resonance imaging (fMRI) and near-infrared optical imaging (NIOI). A tight coupling of these changes has been assumed to elucidate brain function from data obtained with those techniques. In the present study, we investigated the relationship between neuronal activity and hemodynamic responses in the occipital cortex of humans during visual stimulation and in the somatosensory cortex of rats during peripheral nerve stimulation.

Methods: The temporal frequency dependence of macroscopic hemodynamic responses on visual stimuli was investigated in the occipital cortex of humans by simultaneous measurements made using fMRI and NIOI. The stimulus-intensity dependence of both microscopic hemodynamic changes and changes in neuronal activity in response to peripheral nerve stimulation was investigated in animal models by analyzing membrane potential (fluorescence), hemodynamic parameters (visible spectra and laser-Doppler flowmetry), and vessel diameter (image analyzer).

Results: Above a certain level of stimulus-intensity, increases in regional cerebral blood flow (rCBF) were accompanied by a decrease in regional cerebral blood volume (rCBV), i.e., dissociation of rCBF and rCBV responses occurred in both the human and animal experiments. Furthermore, the animal experiments revealed that the distribution of increased rCBF and O_2 spread well beyond the area of neuronal activation, and that the increases showed saturation in the activated area.

Conclusions: These results suggest that above a certain level of neuronal activity, a regulatory mechanism between regional cerebral blood flow (rCBF) and rCBV acts to prevent excess O_2 inflow into the focally activated area.

Background

The existence of coupling between neuronal activity, metabolic and hemodynamic responses is a prerequisite for brain function research employing non-invasive neuroimaging techniques such as functional magnetic resonance imaging (fMRI), positron emission tomography (PET) and near-infrared optical imaging (NIOI), which can visualize stimulus-induced activation areas in the human brain (see Rev. [1]). Although the mechanism of the coupling between these physiological parameters remains to be elucidated despite numerous investigations conducted over past decades (see Rev. [2]), a tight coupling has been assumed to elucidate brain function based on the data obtained using these techniques (see Rev. [3]).

Within the past some dozen years, it has been reported that changes in rCBF in response to visual stimuli are accompanied by smaller changes in the regional metabolic rate of O_2 (rCMRO$_2$) in the human visual cortex (e.g., ΔrCBF: ΔrCMRO$_2$ = 10:1 [4] or 2:1 [5]). This implies that the oxygen supply is not precisely matched with the demand (referred to as "overcompensation" or "decoupling between ΔrCBF and ΔrCMRO$_2$"). More recently, the use of optical techniques to monitor the visual cortex of animals has shown that (1) after onset of a stimulus, the concentration of deoxy-Hb increases first at a focal region in the cortex co-localized with neuronal activation and increased O_2 consumption, and (2) this is followed by a decrease in deoxy-Hb and a large increase in oxy-Hb, which is caused by a delayed but large and less localized increase in rCBF [6-8].

In the course of our studies, we found a decoupling between rCBF and rCBV during visual stimulation in the human occipital cortex [9], although it has been empirically appreciated that an increase in rCBF accompanies an increase in rCBV. The relationship between the two was determined using whole-head measurement [10], which is often used for the analysis of stimulus-induced changes in rCBF and rCBV. On the basis of our results, we propose that some mechanism regulates regional blood flow (rCBF) and blood volume (rCBV) above a certain level of neuronal activity. If the mechanism works as a general rule during regional brain activation, it should occur regardless of type of stimuli, area of cortex, or animal species.

In the present study, we performed two different experiments to test the above hypothesis. First, the relationship between neuronal activity and hemodynamic responses was examined in the human occipital cortex using two types of visual stimuli (a black and white annular checkerboard and a flash-photo stimulus). Secondly, we investigated the relationship in the rat somatosensory cortex when the peripheral nerve was stimulated electrically.

Here, we discuss the commonly observed regulation of oxygen transport during brain activation.

Methods

Human Experiments

Subjects

Six healthy male subjects (24–43 years old) participated in the human experiments. All subjects had normal or corrected-to-normal vision and provided written informed consent. The Communications Research Laboratory approved the experimental protocols. Four of the six subjects participated in NIOI measurements only. A flash-photo stimulator (SLS-2141, Nihon Kohden Kogyo Co. LTD, Japan) was used to provide visual stimuli (temporal frequency at 0.5, 1, 8 and 21 Hz). The time sequence of the experiments consisted of [control (30 sec) + stimulation (30 sec)]. Each of four different frequencies was shown four times in pseudo-random order. During the experiments, subjects sat still on a chair and were required to keep their eyes closed lightly. Simultaneous measurements using fMRI and NIOI were performed on the other two subjects. A black and white annular checkerboard, with a central fixation point and gray background, was used as the visual stimulus (perimacular annulus, 1.2 to 5.8 degrees; angle of each wedge, 10 degrees; number of layers, 5; temporal frequency, 0.5, 1.4, 4.7, and 14 Hz). The time sequence of the experiments consisted of [control (28 sec) + stimulation (28 sec)]. Each of four different reversal frequencies was shown four times in pseudo-random order. During the control and stimulation periods, subjects were required to fixate on a fixation cross in the middle of the checkerboard, and to lie still on his back on a patient table of MRI.

Optical Measurements and Analysis

A 16-channel near-infrared optical imaging system, OPTIM_A, was used to obtain optical images of changes in concentration of hemoglobin (Hb) species in the occipital cortex for simultaneous measurement with fMRI [11]. The system consisted of six optical source units, each having three laser diodes (780, 805, and 830 nm) and six photomultiplier tubes. The source units and detector tubes were connected to glass-fiber bundles for the illumination of incident light and for the collection of reflected light from the head. Combinations of 16 nearest-neighbor pairs of input and output fibers were used to obtain a topographical image covering a 76 × 76 mm area in the occipital region of the head. The pixel size of the NIOI was estimated to be 20 × 20 mm at a source-detector distance of 27 mm. A single-channel near-infrared spectroscopy (OM-100A, Shimadzu Co., Japan) was used to monitor changes in concentrations of Hb species during the flash-photo stimulation. The system consisted of one optical source unit, with three laser diodes (780, 805, and 830 nm), and one photomultiplier tube. Sampling interval of

near-infrared optical measurements was 1 sec. Changes in the Hb species concentration, expressed in an arbitrary unit, (Δ[oxy-Hb], Δ[deoxy-Hb], and Δ[total-Hb] (= Δ[oxy-Hb] + Δ[deoxy-Hb])) from the control conditions were calculated based on a modified Lambert-Beer law [12], using the extinction coefficient of chromophores reported by Matcher et al. [13] as follows.

$$\Delta[\text{oxy-Hb}] = -1.489\Delta Abs_{780} + 0.597\Delta Abs_{805} + 1.485\Delta Abs_{830}$$

$$\Delta[\text{deoxy-Hb}] = 1.855\Delta Abs_{780} - 0.239\Delta Abs_{805} - 1.095\Delta Abs_{830}$$

fMRI Measurements and Analysis
A 1.5 T MRI scanner (Magnetom Vision; Siemens, Germany) was used to obtain blood oxygen level-dependent contrast functional images. Functional images weighted with the apparent transverse relaxation time (T_2^*) were obtained with an echo planar imaging (EPI) sequence (repetition time (TR), 4000 msec; echo time (TE), 55.24 msec; flip angle (FA), 90°; field of view (FoV), 256 × 256 mm^2; matrix size, 64 × 64; slice thickness, 4 mm). Areas of significant activation were determined using SPM99 http://www.fil.ion.ucl.ac.uk. Motion correction and spatial smoothing (three-dimensional Gaussian kernel, 11 mm full width at half maximum) were successively performed for each subject. Areas of activation were determined by a statistical threshold of P < 0.0001 (voxel level) corrected for multiple comparison for the entire search volume). To enable the fMRI and optical signals to be compared, the time series of the fMRI signals were processed as follows. After removing motion artifacts from all the T_2^*-weighted images using Automated Image Registration (AIR, http://bishopw.loni.ucla.edu/AIR3 version 3.0, the time courses of the fMRI signals from the region of interest were obtained using AVS/Express version 3.2 (Advanced Visual Systems Inc., USA).

Animal Experiments
Animal Preparation
All animal experiments were conducted in accordance with our institutional guidelines for the care and use of laboratory animals. Male Wistar rats weighing 190–220 g were purchased from SLC (Shizuoka, Japan) and allowed free access to food and water. The rats were initially anesthetized with urethane (0.8 g/kg body wt. i.p.). They were then tracheotomized, immobilized with pancuronium bromide (2 mg/kg/h), and artificially ventilated with room air. The ventilation was adjusted to maintain arterial blood gas tension in the physiological range. A craniotomy (4 × 5 mm) was performed on the left hemisphere and the dura mater was removed to expose the somatosensory cortex. A pair of needle electrodes was inserted underneath the skin of the plantar and ankle region in the contralateral hindlimb. Except as otherwise noted, the posterior tibial nerve (in part, the peroneal nerve) was

electrically stimulated with a rectangular pulse of 3.8 mA intensity and 0.5 msec duration at 5 Hz. No major changes were detected in the mean arterial blood pressure (110 mmHg ± 5 S.D.) during and after posterior tibial (PT) nerve stimulation.

Measurement of Hemodynamic Parameters
Regional changes in red-blood-cell flow (rRBC$_{Flow}$), velocity (rRBC$_{Veloc}$), and content (rRBC$_{Mass}$) were measured in 12 rats using a laser-Doppler tissue flowmeter (LDF) (FLO-CE1, Omega Flow Inc., Japan) combined with a microscopy system [14]. Signal changes from the surface of the cortex (semiglobular, 500 μm in diameter) were collected at a time constant of 0.5 sec. In separate experiments (5 rats), changes in the diameters (D) of second- and third- branches of the middle cerebral artery (MCA) and RBC velocity (v) in these single pial arterioles were measured using a fiber-optic laser-Doppler anemometer microscope (FLDAM) [15]. The blood-flow rate in individual microvessels was calculated as v* π(D/2)^2.

Measurements of Activation Area and Blood-Flow Distribution
Another five rats were used to acquire digitized images through transmission filters at 577.3 (± 1.2) nm with a charge-coupled device (CCD) camera. The magnitude of absorption change at 577 nm (ΔA_{577}) was calculated in each pixel and color-coded to produce a false-color map. The same rats were then used for the measurement of membrane potential. The exposed cortex was stained with a voltage-sensitive dye JPW-1114 (Molecular Probes, USA) (0.5 mg/ml for 90 min). The hindlimb was electrically stimulated 21 times with a rectangular pulse of 3.8 mA intensity and 0.5 msec duration at a frequency of 0.33 Hz. The fluorescence associated with membrane potential changes was measured with a high-speed CCD imaging system, MiCAM01 (Brain Vision Inc., Japan). For each stimulation, 84 images were acquired at 2 msec intervals, and 21 series of time-course images were averaged.

Results and Discussion
Figure 1 shows the hemodynamic responses measured using NIOI and/or fMRI in human occipital cortex during visual stimulation. Using flash-photo stimulation, the Hb species concentrations measured with NIOI increased from their basal levels, but the increases were minimum at a temporal frequency of 8 Hz (Fig. 1A). The same response tendency was observed in all subjects. This result was the opposite to results obtained using PET [16] or fMRI [17,18], which showed the maximum increase in rCBF in the visual cortex occurred at around 8 Hz. To investigate this discrepancy between changes in Hb species concentrations and rCBF, we performed simultaneous NIOI and fMRI measurements on two subjects using a black/white annular checkerboard (because we were unable to use our photo stimulator in the MRI system) (Fig. 1B). Changes in

A

B
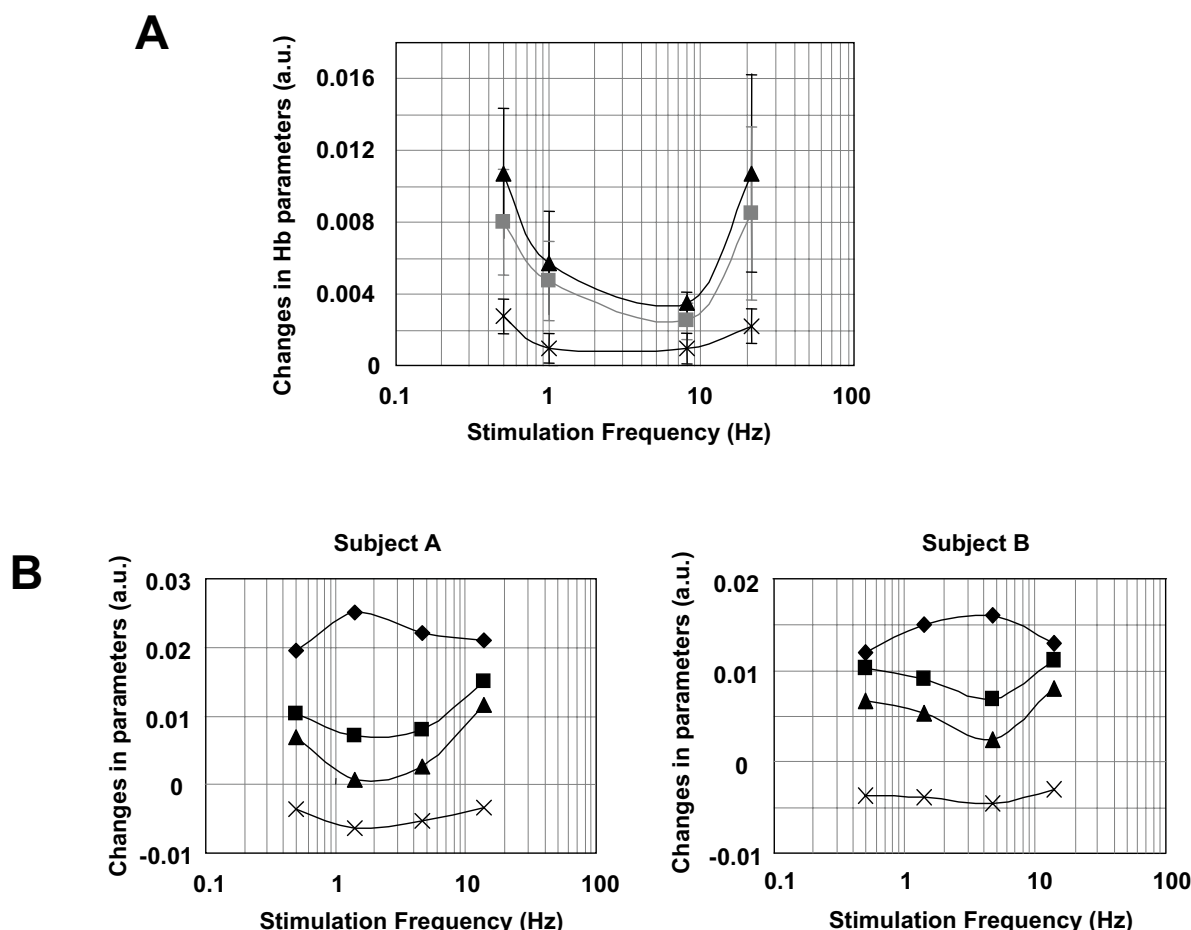
Figure 1
Stimulus-induced hemodynamic responses in human visual cortex. (A) Measurement with NIOI. A flash photo was used for stimulation. Values are mean ± SD (n = 4 subjects). ■, Δ[oxy-Hb] (arbitrary unit); ▲, Δ[total-Hb]; X , Δ[deoxy-Hb] (B) Simultaneous measurement with fMRI and NIOI. The data show subject A (left), B (right), respectively. A black and white annular checkerboard was used as a stimulus. ◆, BOLD signal (%); ■, Δ[oxy-Hb] (arbitrary unit); ▲, Δ[total-Hb]; X , Δ[deoxy-Hb]

the blood oxygenation level-dependent (BOLD) fMRI signals of individual subjects showed a maximum at stimulus frequencies around 1.4–4.7 Hz, while Δ[oxy-Hb], Δ[deoxy-Hb], and Δ[total-Hb] measured with NIOI showed a minimum around these frequencies. It should be noted that the frequency of stimulation using flickering checkerboards is considered to be twice the white-to-white or black-to-black frequency of the checkerboard, if the visual stimulus basically comes from pattern reversal. Thus, the frequency of 1.4–4.7 Hz corresponds to 2.8–9.4 pattern reversals/sec. Therefore, the present results obtained using a checkerboard stimulus are consistent with our NIOI results and the results of other studies obtained using flash-photo stimulation [16-18]. Moreo-

ver, the use of this stimulus highlighted the following two findings: (1) changes in [deoxy-Hb] for the checkerboard stimulation decreased from the basal level (Δ[deoxy] < 0), whereas those for the flash-photo stimulation increased from the basal level (Δ[deoxy] > 0), and (2) the responses of the Hb parameters and BOLD signals dissociated at around 8 Hz. One possible explanation for the former finding is that the difference in the [deoxy-Hb] reflects differences in the metabolic and circulatory conditions in the visual cortex during the resting state. The subjects were asked to close their eyes during the flash-photo stimulation, whereas during the checkerboard stimulation they were asked to keep them open. It has been reported that the metabolic rate of glucose in the visual cortex (CMR-

Glc) decreased from the basal level when subjects closed their eyes, whereas during the checkerboard stimulation (with the eyes open) it increased above the basal level [19]. As for the second finding, the result indicates that the dissociation between rCBF and rCBV occurs at a temporal frequency around 8 Hz, since the temporal frequency dependence of the BOLD signal responses corresponded well with the rCBF responses [16-18], whereas the responses of the Hb parameters, especially [total-Hb], reflected changes in the rCBV. Moreover, it has been reported that electrical [20] and $CMRO_2$ responses [21] showed a maximum at a frequency around 4 Hz (i.e., 8 pattern reversals/sec) when a checkerboard was used for visual stimulation. These results suggest that there are physiological requirements for the dissociation of stimulus-induced responses of rCBF and rCBV above a certain level of neuronal activity.

If the above dissociation phenomenon applies generally to any type of regional brain activation, it should occur regardless of stimulus type, cortical area, or animal species. To test the above hypothesis, we examined stimulus-induced hemodynamic responses in the somatosensory cortex of rats during electrical stimulation of the peripheral nerve (see Materials and Methods). Figure 2 shows the spatiotemporal profile of stimulus-induced activation in the somatosensory cortex of the rat. Figure 2A shows a CCD image over the left parietal cortex viewed through the cranial window. The vessel labeled A is a second-order (parietal) branch of the middle cerebral artery (MCA), and vessels B and C are its tributaries (third-order branches). Vessel B predominantly supplies the hindlimb somatosensory area and vessel C predominantly supplies the trunk area (left branch). One of the tributaries of vessel C formed an interarterial anastomosis with the anterior cerebral artery (ACA), denoted by a broken line. The stimulus-induced maximal neuronal activation obtained with changes in the membrane potential was localized in the hindpaw area at 28 msec after stimulus onset (Fig. 2B, traces 1 and 2). It then propagated over the hindlimb area (Fig. 2B, trace 3). In contrast, Figure 2C shows an absorbance change at a wavelength of 577 nm (ΔA_{577}), which mainly reflects [oxy-Hb], indicating that the change in rCBF spread beyond the hindlimb area at 6 sec after stimulus onset. This wide distribution of CBF correlated well with the widespread increase in intravascular pO_2 measured using albumin-bound oxygen-sensitive phosphorescence dye, although the maximal increases in rCBF and pO_2 were observed over the hindlimb area (Fig. 2D).

Figure 3A shows representative temporal profiles of changes in the hemodynamic parameters measured using LDF in the maximally activated hindpaw area (marked with a white circle in Figs. 2C and 2D), in which maximal changes in RBC flow ($rRBC_{Flow}$), RBC velocity ($rRBC_{Veloc}$),

and RBC number ($rRBC_{Mass}$) were observed 5~7 sec after stimulus onset. To investigate the relationship between stimulus intensity and degree of change in these hemodynamic parameters, the LDF measurements were performed in the activated hindpaw area at various current intensities and stimulus periods (Fig. 3B). Since it has been reported that electrical stimulation of the peripheral nerve of rats showed a maximal response (without tetanus) of the hemodynamic parameters at around 5 Hz [22], the stimulus frequency was kept at 5 Hz during this experiment. The index of stimulus intensity (horizontal axis in Fig. 3B) was assumed as a function of a product of the current intensity and stimulus period. At a lower stimulus intensity (SI ≤ 2), $rRBC_{Flow}$, $rRBC_{Veloc}$, and $rRBC_{Mass}$ all increased (P < 0.001) due to functional hyperemia, while at a higher stimulus intensity (SI > 2), $rRBC_{Flow}$ and $rRBC_{Veloc}$ increased, while $rRBC_{Mass}$ decreased (P < 0.001). These results demonstrated that the dissociative response between rCBF and rCBV in the human visual cortex (Fig. 1) also occurred in the somatosensory cortex of rats in response to different stimuli. This finding strongly suggests that Grubb's relationship between CBF and CBV (CBV = $0.8*CBF^{0.38}$) [10] does not always apply, especially to the relationship between regional changes in CBF and CBV (probably above a certain level of neuronal activation). In addition, the saturation of the increase in $rRBC_{Flow}$ indicates that the maximal level of increase in O_2 inflow into the activated area remains at a certain level (about 30%, see Fig. 3B) because the increased $rRBC_{Flow}$ reflects the inflowing oxygenated RBC.

Figure 4A shows changes in the blood flow rate and diameter (inset) of the pial arterioles supplying the blood to the hindpaw area (see Fig. 2A). The blood flow and diameter of the afferent vessel A and its tributaries (B, which supplies the hindlimb area, and C, which supplies the trunk area) increased just after the onset of stimulation (Fig. 4A), but the pial arterioles lying in other areas remained unchanged. The tissue blood flow in the hindpaw area measured using the laser-Doppler flowmeter increased in accordance with the increase in blood flow in vessel B measured using the FLDAM. The blood flow and diameter of vessel B showed long-lasting increases, probably due to the metabolic effect of the neuronal activation in the hindpaw area. It should be noted that vessel C does not supply blood to the activated area, but the change in blood flow in vessel C was almost the same as that in vessel B. These results suggest that the increases in the diameter and blood flow in vessel C are regulated so that vessel C plays an active role as an "escape route" to prevent excess inflow of O_2 into vessel B. The increase in pO_2 more than 10 mmHg may be undesirable in the capillary bed and venules in the activated area (cf., Fig. 2D). These results may account for the finding that the maximal level of increase in O_2 inflow into the activated area remained
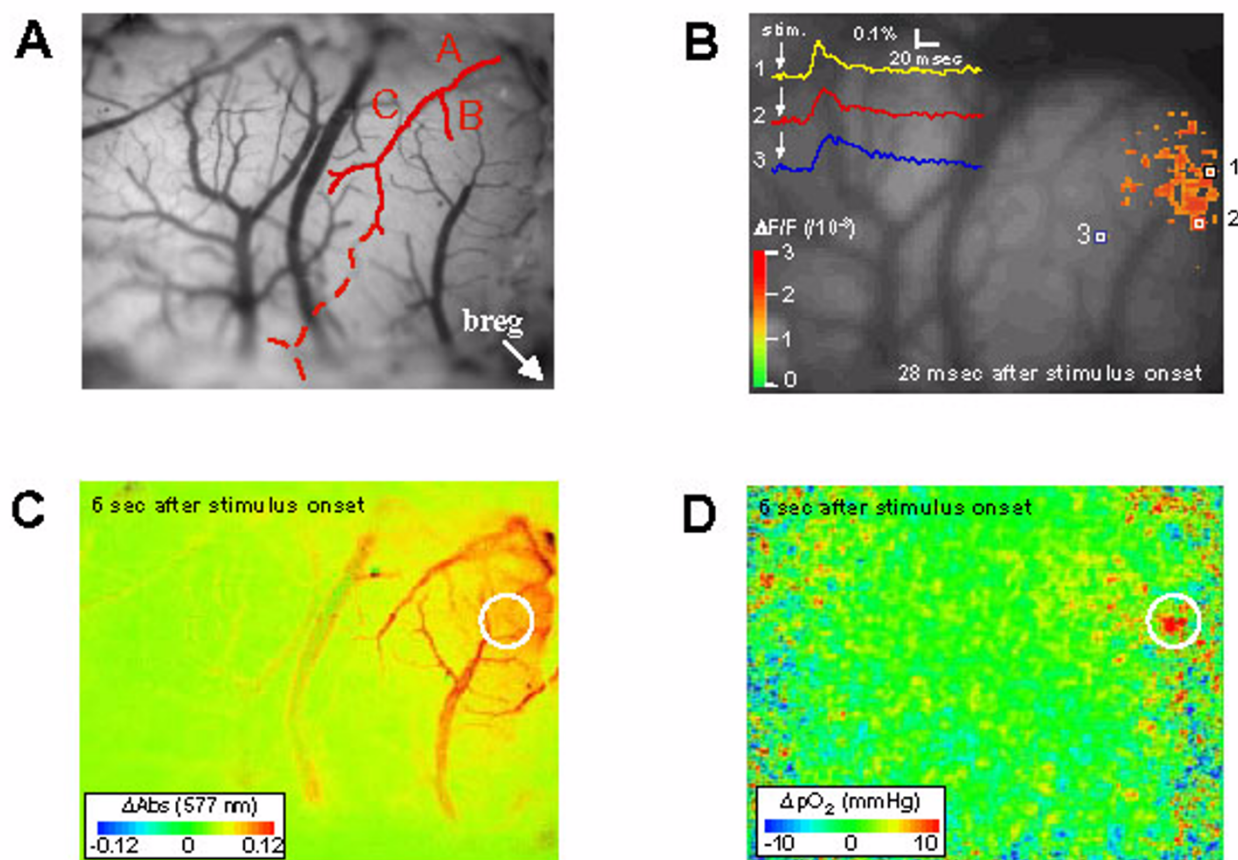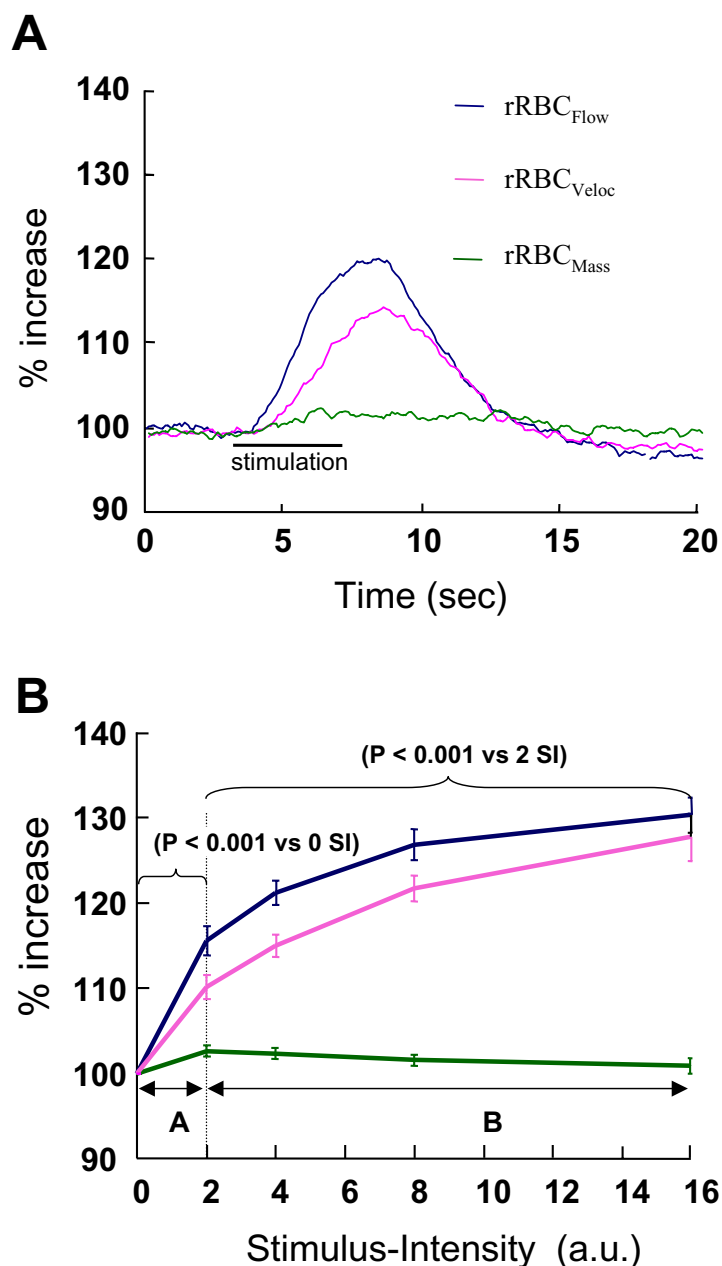
Figure 2
Representative results of optical imaging in the rat somatosensory cortex during PT nerve stimulation. (A) CCD image over the left parietal cortex through the cranial window. The bottom right corner of the figure shows 0.5 mm lateral and 0.5 mm caudal from the bregma. Vessels traced with red solid line denote parietal branches of the MCA, and broken lines denote parietal branches of the anterior cerebral artery (ACA). (B) Stimulus-induced activation area measured using voltage-sensitive dye. The map was obtained above 50% of threshold ($0.15 \leq \Delta F/F$ (%) ≤ 0.3) at 28 msec after stimulus onset. Maximal activation of the somatosensory cortex was observed in the hindpaw area. Time courses of changes in membrane potential at the numbered pixels are superimposed (1 and 2, hindpaw area; 3, hindlimb area). (C) Spatial distribution of stimulus-induced absorption change (ΔA_{577}) at 6 sec after stimulus onset. (D) Maximal spatial distribution of intravascular pO_2 at 7 sec after stimulus onset. The images were 4 × 5 mm. The somatosensory area could be divided into the following four regions [25]: upper right, predominantly hindlimb area; lower right, predominantly motor area; upper and lower left, predominantly trunk area.

at a certain level (i.e., the asymptotic increase in $rRBC_{Flow}$ in Fig. 3). The stimulus conditions used in this study (a rectangular pulse of 3.8 mA intensity and 0.5 msec duration at 5 Hz) considerably exceeded motor and sensory thresholds, which may have been sufficient to excite Aα, Aβ, and Aδ axons and C-fibers [23]. In turn, this may have been enough to elicit the maximal increase in $rRBC_{Flow}$ and a maximal level of O_2 inflow in the hindpaw area [24]. These results are summarized in Fig. 4B. The diameter and blood flow of the afferent vessel A and its tribu-

taries, B and C, increased just after onset of the stimulation due to a fast and transient neurogenic regulation. The blood supply to the activated area was maintained by a delayed and lasting metabolic factor. Vessel C does not supply blood to the activated area, but the change in blood flow in vessel C (27% increase) was almost the same as that in vessel B (30% increase), suggesting that vessel C plays an active role as an "escape route" to prevent excess O_2 inflow into vessel B and the activated area. This regulation could be achieved by a dis-

A

B

Figure 3
Changes in hemodynamic parameters in the hindpaw area during PT nerve stimulation. (A) Typical example of temporal profiles of stimulus-induced changes in hemodynamic parameters measured using LDF. Measurements focused on the hindpaw area shown with a white circle (500 μm in diameter) in Figs 2(C) and 2(D). The horizontal bar denotes the stimulus period (4 sec). (B) Changes in hemodynamic parameters as a function of stimulus intensity. Vertical axis denotes percent increases in tissue blood flow ($rRBC_{Flow}$), red blood cell velocity ($rRBC_{Veloc}$), and number of red blood cells ($rRBC_{Mass}$) in the hindpaw area measured with LDF. Horizontal axis denotes index of stimulus intensity as a function of stimulus duration (2, 4 or 8 sec) and current intensity (2.5, 5, 7.5 or 10 mA). Other stimulus conditions were pulse duration of 0.5 msec and stimulus frequency of 5 Hz. Each data point represents 36 measurements from 12 rats. Statistical analysis was done using a Bonferroni multiple comparison test, and $P < 0.05$ was regarded as statistically significant.
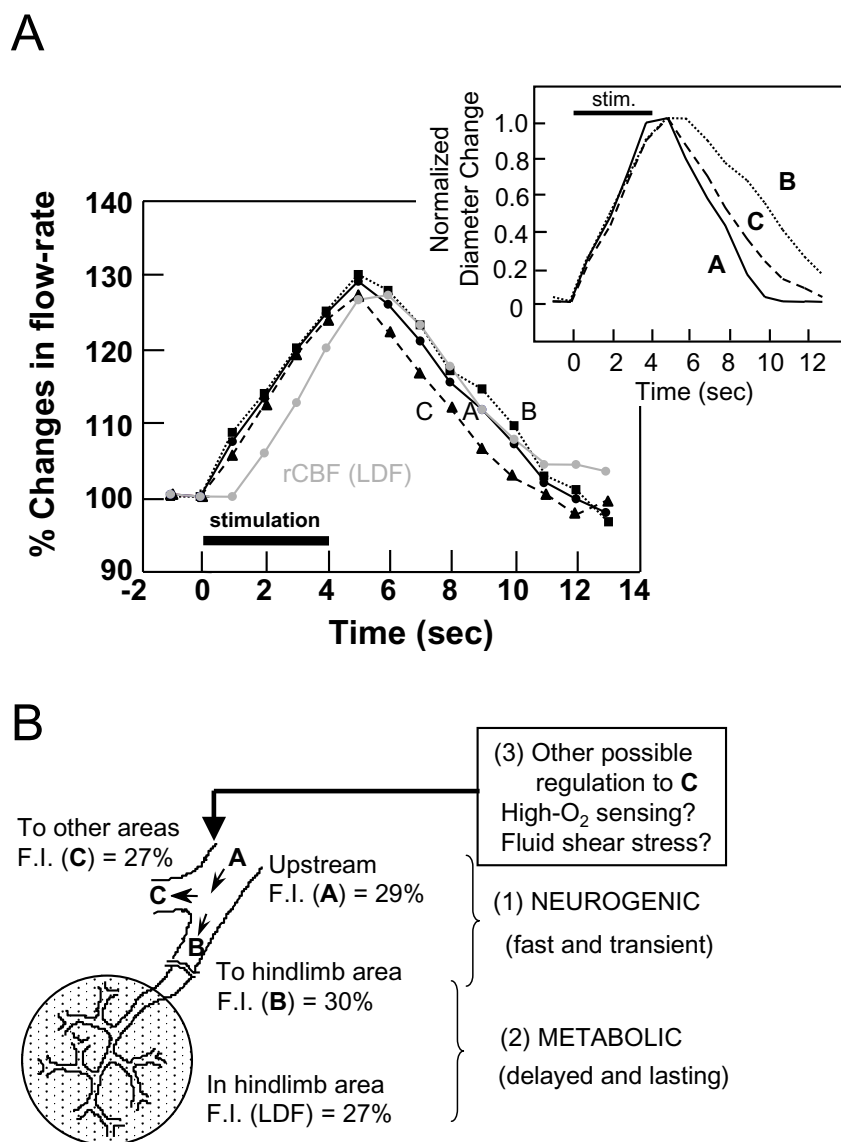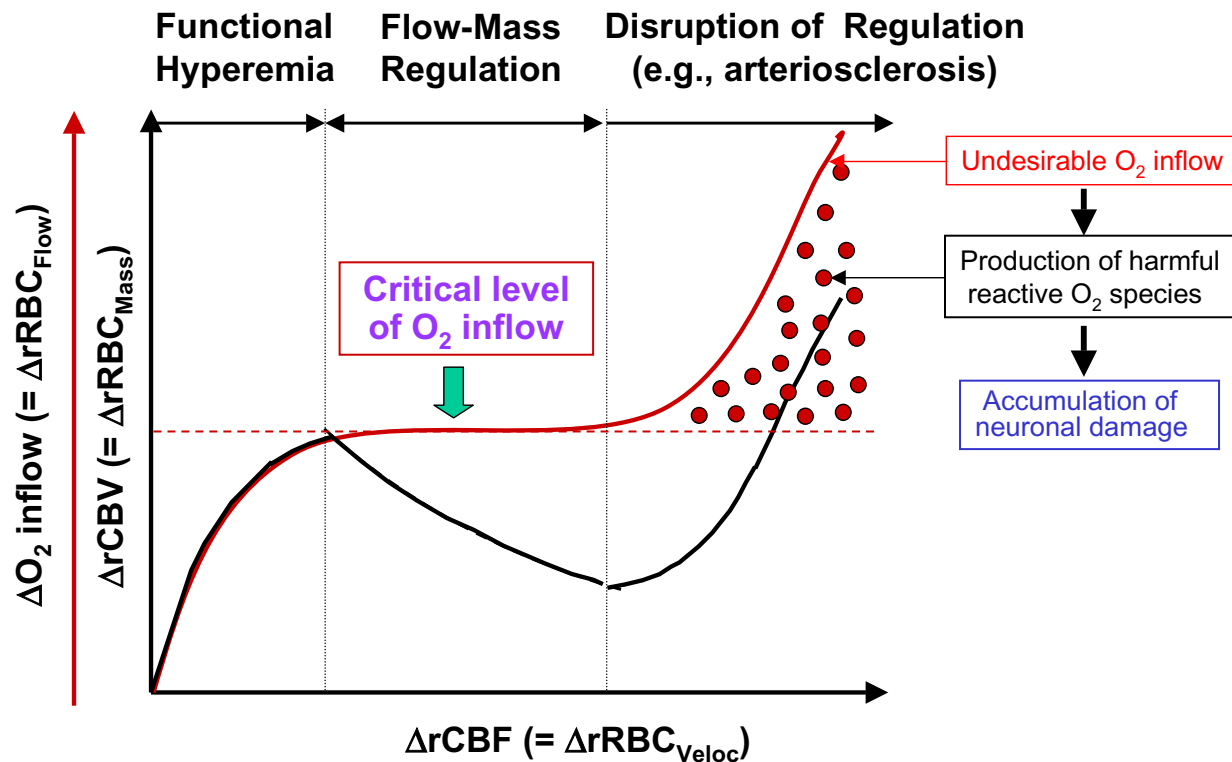
Figure 4
Stimulus-induced changes in pial arteriolar blood flow and diameter in the somatosensory cortex. (A) Comparison of the time course of rCBF measured using LDF and blood-flow rate in individual pial arterioles measured using FLDAM. Vessels labeled A are second-order branches of MCA (32.7 μm ± 14.3 SD in diameter), those labeled B are third-order branches (25.0 μm ± 11.3 SD) supplying the hindlimb (hindpaw) somatosensory area, and those labeled C are third-order branches (24.3 μm ± 11.1 SD) predominantly supplying the trunk area (see Fig. 2A). Normalized time course-changes in diameter are shown in the inset. Averaged values from 15 trials of 5 rats are shown; the errors for each data point are less than 10%. (B) Illustration of blood-flow regulation in the somatosensory cortex during PT nerve stimulation. F.I. denotes flow increase. The flow data shown were from (A).

Figure 5
Scheme of hypothetical blood-flow regulation during brain activation. Relationship between ΔrCBV and ΔrCBF in the activated area is shown by black line. Relationship between ΔO_2 inflow and ΔrCBF in the activated area is shown by red line. During moderate neuronal activation, rCBF, rCBV and O_2 inflow increase in the activated area (functional hyperemia). Above a certain level of neuronal activation, dissociation of increase in rCBF and rCBV takes place to prevent excess O_2 inflow into the focally activated area (Flow-Mass regulation). Normal regulation of rCBF and rCBV is probably achieved by the action of both regulations (i.e., functional hyperemia and Flow-Mass regulation). Further, we hypothesize that when Flow-Mass regulation is disrupted (e.g., arteriosclerosis), rCBF, rCBV, and O_2 inflow may increase to undesirable levels in the activated area, leading to the production of harmful reactive oxygen species resulting in accumulation of neuronal damage.

sociation between rCBF and rCBV responses, called a flow-mass regulatory mechanism. A third mechanism, possibly a high-O_2 sensing mechanism and/or fluid shear stress, may act as a regulator for the mechanism in addition to the neurogenic and metabolic regulation.

In conclusion, our results indicate the existence of a flow(rCBF)-mass(rCBV) regulatory mechanism, and that changes in blood flow during brain activation are not tightly regulated to supply only to an the activated area. This loose regulation serves to prevent intense functional hyperemia and excess O_2 inflow into the focally activated area. A high-O_2 sensing mechanism and/or fluid shear

stress are proposed as a regulator of the flow-mass regulatory mechanism, which may elicit a neurogenic modulation of vascular tonus in the activated cortex. Collapse of the flow-mass regulatory mechanism (e.g., arteriosclerosis) would result in excess inflow of oxygen into the focally activated area, triggering the production of harmful reactive oxygen species and leading to the accumulation of irreversible neuronal damage (Fig. 5).

Authors' contributions
AS conceived, designed and coordinated the study, participated in all the human and animal experiments, and drafted the manuscript. JS participated in the design and

coordination of the study, and carried out the FLDAM measurements. HCT participated in designing the human experiments and carried out the fMRI measurements. YO participated in all the animal experiments. YS participated in the LDF measurements for the animal experiments. HF participated in the design and coordination of the animal experiments. TY participated in the design and coordination of the study, and directed it. All authors read and approved the final manuscript.

Acknowledgements

References

1. Villringer A: **Physiological changes during brain activation.** In: *Functional MRI* Edited by: *Moonen CT, Bandettini PA. Berlin, Springer*; 1999:3-13.
2. Raichle ME: **Behind the scenes of functional brain imaging: A historical and physiological perspective.** *Proc Natl Acad Sci USA* 1998, **95:**765-772.
3. Raichle ME: **Circulatory and metabolic correlates of brain function in normal humans.** In: *Handbook of Physiology: The Nervous System V: Higher Functions of the Brain* Edited by: *Plum F, Bethesda MD. Am Physiol Soc*; 1987:643-674.
4. Fox PT, Raichle ME, Mintun MA, Dence C: **Nonoxidative glucose consumption during focal physiologic neural activity.** *Science* 1988, **241:**462-464.
5. Hoge RD, Atkinson J, Gill B, Crelier GR, Marrett S, Pike B: **Linear coupling between cerebral blood flow and oxygen consumption in activated human cortex.** *Proc Natl Acad Sci USA* 1999, **96:**9403-9408.
6. Malonek D, Grinvald A: **Interactions between electrical activity and cortical microcirculation revealed by imaging spectroscopy: Implications for functional brain mapping.** *Science* 1999, **272:**551-554.
7. Malonek D, Dirnagl U, Lindauer U, Yamada K, Kanno I, Grinvald A: **Vascular imprints of neuronal activity: Relationships between the dynamics of cortical blood flow, oxygenation, and volume changes following sensory stimulation.** *Proc Natl Acad Sci USA* 1997, **94:**14826-14831.
8. Vanzetta I, Grinvald A: **Increased cortical oxidative metabolism due to sensory stimulation: Implications for functional brain imaging.** *Science* 1999, **286:**1555-1558.
9. Seiyama A, Tanabe HC, Sase I, Eda H, Seki J, Yanagida T: **Hemodynamic response during visual stimulation in humans: Comparison between near-infrared optical imaging and functional magnetic resonance imaging.** *XXXIV IUPS Abstract CD-ROM* 2001, **Abst ID No. 502:**.
10. Grubb RL, Raichle ME, Eichling JO, Ter-Pogossian MM: **The effects of changes in $PaCO_2$ on cerebral blood volume, blood flow and vascular mean transit time.** *Stroke* 1974, **5:**630-639.
11. Sase I, Eda H, Seiyama A, Tanabe HC, Takatsuki A, Yanagida T: **Multichannel optical mapping: Investigation of depth information.** *Proc SPIE* 2001, **4250:**29-36.
12. Eda H, Sase I, Seiyama A, Tanabe HC, Imaruoka T, Tsunazawa Y, Yanagida T: **Optical topography system for functional brain imaging: Mapping human occipital cortex during visual stimulation.** In: *Proceedings of Inter-Institute Workshop on In Vivo Optical Imaging at the NIH* Edited by: *Gandjbakhche AH, Bethesda MD. Optical Soc. America*; 2000:93-99.
13. Matcher SJ, Elwell CE, Cooper CE, Cope M, Delpy DT: **Performance comparison of several published tissue near-infrared spectroscopy algorithms.** *Anal Biochem* 1995, **227:**54-68.
14. Seiyama A, Shiga T: **Oxygen transfer in peripheral organs: Researches on intact organs with optical techniques.** *Adv Exerci Sports Physiol* 1998, **4:**37-49.
15. Seki J, Sasaki Y, Oyama T, Yamamoto J: **Fiber-optic laser-Doppler anemometer microscope applied to the cerebral microcirculation in rats.** *Biorheology* 1996, **33:**463-470.
16. Fox PT, Raichle ME: **Stimulus rate dependence of regional cerebral blood flow in human striate cortex, demonstrated by positron emission tomography.** *J Neurophysiol* 1984, **51:**1109-1120.
17. Kwong KK, Belliveau JW, Chesler DA, Goldberg IE, Weisskoff RM, Poncelet BP, Kennedy DN, Hoppel BE, Cohen MS, Turner R, Cheng H-M, Brady TJ, Rosen BR: **Dynamic magnetic resonance imaging of human brain activity during primary sensory stimulation.** *Proc Natl Acad Sci USA* 1992, **89:**5675-5679.
18. Thomas CG, Menon RS: **Amplitude response and stimulus presentation frequency response of human primary visual cortex using BOLD EPI at 4 T.** *Magn Reson Med* 1998, **40:**203-209.
19. Phelps ME, Mazziotta JC, Kuhl DE, Nuwer M, Packwood J, Metter J, Engel JrJ: **Tomographic mapping of human cerebral metabolism: Visual stimulation and deprivation.** *Neurology* 1981, **31:**517-529.
20. Adachi-Usami E: **Human visual system modulation transfer function measured by evoked potentials.** *Neurosci Lett* 1981, **23:**43-47.
21. Vafaee MS, Meyer E, Marrett S, Paus T, Evans AC, Gjedde A: **Frequency-dependent changes in cerebral metabolic rate of oxygen during activation of human visual cortex.** *J Cereb Blood Flow Metab* 1999, **19:**272-277.
22. Matsuura T, Fujita H, Seki C, Kashikura K, Yamada K, Kanno I: **CBF change evoked by somatosensory activation measured by laser-Doppler flowmetry: Independent evaluation of RBC velocity and RBC concentration.** *Jpn J Physiol* 1999, **49:**286-296.
23. Sato A, Kaufman AK, Koizumi K, Brooks CM: **Afferent nerve groups and sympathetic reflex pathways.** *Brain Res* 1969, **14:**575-587.
24. Fehlings MG, Tator CH, Linden RD, Piper IR: **Motor and somatosensory evoked potentials recorded from the rat.** *Electroenceph Clin Neurophysiol* 1988, **69:**65-78.
25. Hall RD, Lindholm EP: **Organization of motor and somatosensory neocortex in the albino rat.** *Brain Res* 1974, **66:**23-38.